Sound & Vibration 2026, 60(6), 4694.
doi: https://doi.org/10.59400/sv4694

Article

Vibro-dynamic testing of a 6-story building and reliability assessment taking into account deformation nonlinearity

Yerken Aldakhov[1], Zhassulan Omarov[1], Kulyanda Turekulova[2], Vladimir Lapin[2,*]

[1] Kazakh Research and Design Institute of Construction and Architecture JSC, Almaty 050000, Kazakhstan; ealdakhov@kazniisa.kz (YA); zomarov@kazniisa.kz (ZO)

[2] National Scientific Center for Seismological Observations and Research LLP, Almaty 050060, Kazakhstan; kulyanda@mail.kz

*** Corresponding author:** Vladimir Lapin, lapin_1956@list.ru

CITATION

Aldakhov Y, Omarov Z, Turekulova K, et al. Vibro-dynamic testing of a 6-story building and reliability assessment taking into account deformation nonlinearity. Sound & Vibration. 2026; 60(6): 4694. https://doi.org/10.59400/sv4694

ARTICLE INFO

Received: 17 July 2026
Revised: 21 August 2026
Accepted: 25 March 2026
Available online: 24 September 2026

Abstract: The paper presents the results of vibro-dynamic testing of a 6-story residential building constructed in an area with a seismic intensity of 10 points. The novelty of the study lies in the full-scale testing of a six-story monolithic building and the subsequent use of the test results to calculate reliability as the probability of failure-free performance. The results obtained make it possible to predict the behavior of the building under seismic action. Structurally, the investigated building is a spatial cross-wall system. The basement and above-ground floors are made of monolithic reinforced concrete structures. The dynamic loading is generated by an inertial vibration machine. Vibration measurements were carried out using a digital instrumentation and measurement system. It is shown that the building deforms nonlinearly. The stiffness of the "test object–foundation" system decreased by a factor of 2.14 compared with its initial stiffness, while the stiffness of the object's "structural system" decreased by a factor of 1.37. The dissipative forces of the building were studied. The logarithmic decrement of vibration was constant and equal to 0.46. The coefficient of nonlinearity changed approximately twofold. Based on experimental deformation diagrams, the reliability W (probability of failure-free operation) of the building was calculated. For this purpose, the statistical simulation method (Monte Carlo method) was applied. Reliability and failure values were obtained for three values of internal viscous friction. The accuracy of determining reliability and failure values was assessed by studying the convergence of the process with an increasing number of artificial accelerograms. The results allow the building to be considered seismically resistant at high acceleration values at the foundation.

Keywords: vibro-dynamic loading; reliability; nonlinearity; decrement; period; stiffness

1. Introduction

The global seismic situation is entering a new stage. On June 24, 2026, earthquakes occurred simultaneously in three different parts of the world: a magnitude 5.6 earthquake in California, a 7.2 tremor in Japan, and a double earthquake in Venezuela with magnitudes of 7.2 and 7.5. All three seismic events occurred within a short period of no more than 8 h, sparking online speculation about their possible connection. The connection between these events can be debated at length, but it is undeniable that the global seismic situation is becoming more complex.

A magnitude 7.8 earthquake occurred on the night of February 6 in Turkey and Syria [1,2]. Within 24 h, powerful aftershocks with a magnitude of at least 6 followed, one of which reached 7.5. The cities of Gaziantep, Kahramanmaraş, and Antakya suffered extensive damage. Approximately 62,000 people lost their lives, more than 120,000 were injured, and millions were left homeless.

On September 8, 2023, a magnitude 6.8 earthquake occurred in Morocco within the High Atlas mountain range [3,4]. The earthquake was felt in major cities throughout the country, including Marrakesh, where numerous historic buildings were damaged. Nearly 3,000 people died.

On October 7, 2023, a series of earthquakes with magnitudes reaching 6.4 occurred near Herat, Afghanistan [5]. The disaster resulted in 2,530 fatalities and 9,240 injuries. Even the smaller earthquake that struck Afghanistan on August 31, 2025, with a magnitude of $M_W = 6.1$, caused more than 2,200 deaths and over 4,000 injuries [6].

Thus, strong earthquakes have caused the deaths of large numbers of people in both urban and rural areas. This led to the rapid development of experimental methods for investigating the behavior of buildings under strong dynamic excitations of a seismic nature. Researchers focused their attention on the use of inertial vibration machines.

Vibration testing is an important method for testing all types of buildings, including monolithic buildings. An inertial vibration machine is installed on the roof of the building, and resonant vibrations of the building are excited. Although such actions are not seismic, they are extremely useful because they make it possible to determine changes in the dynamic characteristics of buildings depending on the loading level, identify building damage patterns, establish the drift values at which particular degrees of building damage occur, etc.

Historically, such vibro-dynamic tests began to be conducted in the former Soviet Union in the early 1970s [7]. Subsequently, hundreds of vibro-dynamic tests were carried out, yielding significant results for various types of buildings. Examples of such tests are presented in the comprehensive study on the seismic resistance of monolithic buildings [8].

A typical study is presented in Zolotkov [9]. Two six-story fragments of monolithic buildings were constructed for vibro-dynamic testing. Both fragments were brought to failure. The damage reached Grade 4. At this stage, the tests were discontinued, and both fragments were strengthened using polymer compositions. This experiment made it possible to refine the computational models of monolithic buildings, validate the previously developed analytical method for calculating them with allowance for seismic action, experimentally verify the effectiveness of various wall reinforcement systems used in monolithic buildings, and trace changes in their dynamic characteristics as plastic deformations and various types of damage developed in the structures.

Among the most recent studies based on the results of vibro-dynamic testing, work [10] should be noted. Based on vibration testing, the seismic resistance of a 25-story monolithic residential building in Almaty, located at a site with a seismic intensity of 9 points, was assessed.

An interesting method involving the use of microvibrations is proposed in Hadianfard et al. [11]. The vibrations of four different buildings—two framed and two monolithic—were recorded during construction at three independent stages: erection of load-bearing structures, installation of partitions, and construction of façades and parapets. Two signal-processing methods were used. The vibration periods and frequencies of the buildings were then determined at all stages of construction.

For high-rise monolithic buildings in China, regression relationships for the vibration periods of these structures were obtained based on measurements of microseismic vibrations [12]. Using highly sensitive sensors, a signal converter, and data-acquisition equipment in combination with random-signal processing methods, the vibration periods along two horizontal axes, mode shapes, and dissipative characteristics were determined. Tests conducted on 50 high-rise monolithic wall structures ranging from 30 to 80 m in height in a seismically active region of Northern China yielded formulas for determining these characteristics as functions of height. These formulas are highly useful for practical design applications.

In Wajima, traditional wooden houses, which are common throughout the region, suffered significant damage, many of which completely collapsed. Modern buildings, although designed for earthquake resistance, also suffered damage, especially non-load-bearing elements such as walls, windows, and roofs [13]. Numerous temples, shrines, and cultural heritage sites located throughout the region were affected, with some structures partially or completely destroyed. Many elderly people living in traditional, older homes suffered disproportionately from the earthquake. These structures, often not upgraded to modern seismic standards, suffered significant damage, leaving many elderly people homeless or in unsafe conditions.

Thus, in recent years, significant seismic events have occurred, resulting in large numbers of deaths. This applies to both fairly developed countries and economically weak countries. Therefore, it is necessary to conduct scientific research related to both experimental studies of buildings of various types and theoretical studies of their reliability.

Reliability theory methods are widely applied in the analysis and design of building and structural systems subjected to both static and dynamic loads [14], including structures exposed to seismic impacts [15]. In Lapin et al. [16], an efficient reliability assessment method for framed buildings was proposed based on modeling seismic excitation as a stochastic process represented by a non-canonical spectral formulation. The reliability of large-panel buildings in Aldakhov et al. [17] was calculated using the statistical testing method (the Monte Carlo method).

A comprehensive review of various Monte Carlo approaches is presented in Hurtado and Barbat [18]. Four groups of methods were identified: (1) statistical variability of parameters, in which uncertain parameters are considered as random variables; (2) methods incorporating spatial variability of random parameters; (3) advanced Monte Carlo techniques developed for estimating extremely low failure probabilities; and (4) the response surface method. The limits of their applicability have been identified. The study by Hofer et al. [19] analyzes the principal sources of uncertainty involved in both seismic hazard assessment and structural vulnerability analysis and investigates their influence on the variability of the resulting reliability index.

Based on probability density evolution theory, Shen et al. [20] analyze structural damage and the reliability of a reinforced concrete frame structure under random ground motion conditions caused by a sequence of main and subsequent aftershocks. The randomness of seismic vibrations and structural parameters is taken into account, and the impact of aftershocks on the reliability of the structure is examined. Nonlinear dynamic models for reliability assessment were studied in Brenner and Bucher [21].

For problems of assessing the reliability and seismic resistance of buildings, regional consideration of seismic impact is highly desirable [22].

Buildings constructed on unfavorable sites in seismic regions are classified by the building codes of the Republic of Kazakhstan and the Eurocodes as structures of increased importance, possessing specific characteristics that distinguish them from buildings located on favorable seismic sites.

Such buildings may be categorized as structures with a special level of responsibility.

Their distinctive features are associated with the following requirements:

- The design is developed directly according to special technical specifications (hereinafter referred to as STS);
- This STS document is also required in cases where it is impossible to meet certain requirements of current regulatory documents during the design process.

The design and construction of buildings on unfavorable sites in seismic regions constitute a complex engineering challenge. Its proper solution is possible only through the application of appropriate STS provisions, supported by specialized technical resources, construction technologies, and comprehensive experimental investigations.

Given the complexity of calculations and design for buildings located on unfavorable construction sites, this is entirely understandable, as regulations, in their traditional form, establish requirements only for standard situations and do not cover special cases, which are subject to consideration in specialized regulatory and instructional documents or in targeted technical specifications.

In technical specifications, this strategy is implemented as follows:

Differences between the calculated seismic loads adopted when designing buildings on unfavorable construction sites and the actual seismic loads corresponding to rare strong earthquakes are compensated for by special structural measures.

The special structural measures specified in the special technical specifications were developed on the basis of an analysis of current design standards, experimental and theoretical studies conducted in Kazakhstan and abroad, and practical experience gained from the construction of such buildings in the seismic regions of the Republic of Kazakhstan.

At the same time, work on regulating the basic design principles for buildings on unfavorable construction sites in seismic zones cannot be considered fully complete. A number of conceptual questions remain, the answers to which can only be obtained by accumulating and generalizing experimental data on the actual performance of buildings under seismic loads.

Based on the nature and characteristics of seismic impacts, the most preferable are experimental studies, during which the dynamic nature of loading of the objects under study is realized.

These experiments make it possible to obtain objective information regarding the effectiveness of adopted structural solutions, including systems and structural components that have not previously been verified under real earthquake conditions. In addition, they provide valuable data for evaluating and validating the computational models used in seismic-resistant design and reliability assessment of structural systems.

The main objective of the completed research work was to study the specific behavior of a 6-story residential building's wall structural system under seismic loads and to verify the correctness of the calculation assumptions adopted during its design. The reliability assessment was aimed at obtaining a quantitative evaluation of the building's seismic performance and earthquake resistance.

The objectives of the experimental studies of the 6-story building included:

- Determining the degree of agreement between the measured dynamic characteristics of the building (natural periods and mode shapes) and the corresponding analytical predictions;
- Evaluating the energy dissipation properties of the multi-story structure;
- Investigating the structural response of the building under dynamic loads;
- Assessing the ductility coefficient of the structure;
- Assessing the ability of floor slabs to distribute horizontal seismic loads between vertical load-bearing elements.

The objective of an experimental study of the seismic resistance of a 6-story building made of wall structures on a 10-point construction site has not previously been addressed. Therefore, the conducted research represents a significant innovation. The research results will contribute to the development of earthquake-resistant construction in areas with high-magnitude potential for earthquakes. Historical earthquakes with magnitudes of 8.2–8.3 [23] are known in Almaty: Chilik, 11.07.1889; Kemin, 03.01.1911.

2. Materials and methods

2.1. Brief description of the construction site

For the experimental investigation, Altyn Sapa NS LLP provided a 6-story residential building under construction within the Arena Park Standart 1 residential complex in Almaty.

The construction site has a seismicity rating of 10 points. The soil seismicity category is third (IIIrd).

The building is designed with 1 basement floor and 6 above-ground residential floors.

The construction site is characterized by the following engineering, geological, and seismological conditions:

Geomorphologically, the site is located within a foothill plain, on the third floodplain terrace of the Bolshaya Almatinka River. The site's surface slopes generally northwestward, with absolute ground elevations ranging from 749.8 to 750.7 m.

The geological and lithological structure of the site consists of alluvial-proluvial deposits of the Upper Quaternary age, consisting of loams, sands, and gravel, overlain by a topsoil layer to a depth of 20.0 m.

The topsoil consists of dark-brown, hard loam with plant roots, 0.1–0.3 m thick.

Loams exposed in the upper part of the section down to the groundwater level (GWL) are brownish-gray in color, loess-like, and of a hard to semi-hard consistency, with thin interlayers and lenses of sand and sandy loam (sand lenses and interlayers up to 0.4 m thick), including calcareous clay concretions (crane nodules). The loam layer is 6.0–8.5 m thick.

Light brown loams, ranging from hard and semi-hard to refractory (sometimes soft-plastic and flowing), with inclusions of calcareous-clayey concretions and ferruginous spots, interlayers and lenses of sand. The loam thickness ranges from 3.6 to 12.8 m.

Gray sands, predominantly medium-sized, less commonly fine and coarse, densely packed, with up to 10% gravel and pebbles, ranging from slightly saturated to saturated, with a thickness of 1.3 to 4.7 m.

The gravelly soil consists of a sandy matrix containing approximately 41.4% pebbles, 19.1% gravel, and 39.5% sandy filler. The filler material is predominantly medium-grained sand. The explored thickness of the gravelly layer ranges from 0.8 m to 3.5 m.

During the survey period (October 2023), groundwater levels at the site were detected at depths of 7.2–8.5 m. According to monitoring data, the maximum groundwater level is observed in March-April and the minimum in December–February, with fluctuations of 1.5 m.

Based on the results of engineering-geological surveys and SP RK (Code of Practice of the Republic of Kazakhstan) 2.03-31-2020* [24], when designing the object, the following design parameters were adopted:

- Pebble soil with sand filler;
- Seismic hazard of the construction zone—nine (9) points;
- Type of soil conditions of the construction site according to seismic properties —third (IIIrd);
- Specified seismicity of the construction site—ten (10) points;
- Calculated horizontal acceleration $a_g = 0.66g$, calculated vertical acceleration $a_g = 0.59g$.

2.2. Summary of the space-planning solution

General views of the 6-story residential building of the Arena Park Standard 1 residential complex are presented in **Figure 1**.

The principal design space-planning and structural solutions of the test object are shown in **Figure 2**. The building consists of a single section and has a rectangular floor plan measuring 29.0 m × 12.8 m. The design height of the building from the finished ground level to the roof is 22.2 m.

Figure 1. General views of the 6-story residential building of the Arena Park Standard 1 residential complex.

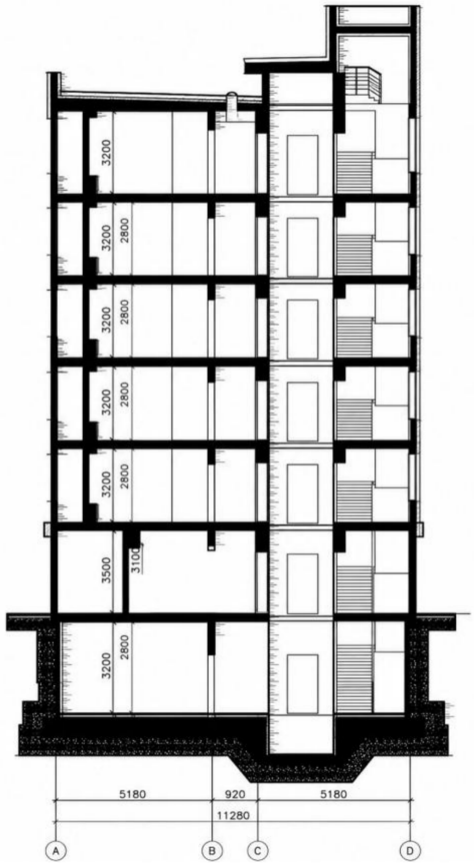

Figure 2. Section 1-1 of a 6-story residential building.

Structurally, the test object is a spatial cross-wall system.

The basement and above-ground floors of the building are constructed of monolithic reinforced concrete structures.

The thickness of the main reinforced concrete walls of the building under study is variable, with a basement thickness of 300 mm and an upper-floor thickness of 200 mm.

Under horizontal loading, the interaction between the reinforced concrete walls is ensured by rigid floor diaphragms. The floor slabs are monolithic reinforced concrete elements with a thickness of 200 mm.

The monolithic reinforced concrete foundation slab is 600 mm thick.

The design concrete strength of all reinforced concrete structures is C20/25 (B25).

The partitions in the building were made of D500 gas blocks, 200 mm and 100 mm thick, and splitter blocks, 190 mm thick, in the basement (see **Figures 3** and **4**).

Figure 3. General design solutions for non-load-bearing structures.

Figure 4. General design solutions for non-load-bearing structures.

Buildings with wall structural systems, due to their technical and economic advantages, great potential for architectural expressiveness in appearance, and wide possibilities for flexible room layouts, have become widely used in earthquake-resistant construction in Almaty.

Analysis of the effects of strong earthquakes and previous tests shows that wall structural systems offer a number of undeniable advantages over framed systems.

Properly designed reinforced concrete walls contribute to:

- A reduction in the amplitude of building vibrations and the associated adverse structural, operational, technological, and socio-psychological effects;
- A significant reduction in the forces in columns and their junctions with adjacent elements due to horizontal loads;
- An increase in the dissipative properties of the structural system;

- A reduction in damage to non-load-bearing elements (partitions, frame infills, stained-glass windows) and utility lines.

The design of the 6-story building was carried out in accordance with the requirements of the standards of the Republic of Kazakhstan SP RK 2.03-30-2017* [25] and the "Special technical specifications (hereinafter referred to as STS) for the design of a multi-story residential complex" (No. 49 dated 18.03.2024).

The design and structural requirements for ensuring the anti-seismic reliability of the building in question, specified in the STS, were developed taking into account its high number of storeys and the specific features of its plan.

In accordance with the provisions of the technical specifications:

a) The building design was carried out taking into account the spatial nature of seismic impacts;
b) In order to reduce damage to non-load-bearing elements (partitions, enclosing walls, etc.), the values of the calculated distortions of floors caused by the impact of calculated seismic loads on the building were limited;
c) The selection of the geometric dimensions of the vertical load-bearing elements of the building (wall thicknesses and column cross-sections) was carried out on the condition of not exceeding the maximum permissible percentage of their longitudinal reinforcement (4%);
d) The anchorage and overlap lengths of the reinforcing bars, and the joined vertical bars, may be allowed to overlap without welding. The required lap splice lengths were determined in accordance with Clause 9.4 of NTP RK (Technical Design Standards of the Republic of Kazakhstan) 02-01-1.1-2011 to SP RK EN 1992-1-1: 2004/2011, Design of Concrete Structures—Part 1-1: General Rules and Rules for Buildings;
e) The space frame clamps installed in the peripheral zones of the wall zones were located:
    - From the foundation edge level to a level of approximately 1/3 of the building's height—with a pitch of no more than 150 mm;
    - Thereafter—with a spacing of no more than 250 mm.
f) In the peripheral zones of the walls adjacent to horizontal technological joints at the top and bottom, the stirrup spacing did not exceed 100 mm;
g) The vertical bars of the reinforcement cages of the peripheral wall zones (at least every other one) were located at stirrup bends, and these bends were spaced no more than 200 mm apart.

The above summary of the principal design and detailing requirements demonstrates that the provisions contained in the STS substantially supplement the standard code requirements and contribute to improving the seismic resistance and reliability of the building.

By the time of testing the experimental object, 1 basement floor and 6 above-ground floors had been erected.

2.3. Preliminary assessments of design solutions

The overall structural design of the full-scale test object was required to comply with the provisions established by the applicable regulatory documents of the Republic of Kazakhstan.

Based on the information provided by Altyn Sapa NS LLP, it was established that within the structural design process:

- At least the consideration of the permanent design situation, as well as the related structural analysis, was carried out in accordance with the provisions of the Code of Practice of the Republic of Kazakhstan [24,25] and other regulatory documents in force at the time;
- The consideration of the seismic design situation, as well as the related structural analysis, was carried out primarily in accordance with the requirements of SP RK 2.03-30-2017* [25] and taking into account the applicable provisions of other regulatory documents.

2.4. Summary of the structural calculations (structural analysis)

During the review of the architectural and structural design solutions adopted for the representative residential building at the selected construction site, information regarding the results of the structural calculations was examined.

The structural analysis, taking into account the seismic design situation, was performed using the Lira SAPR-2022 software package.

The calculation of a 6-story building with a basement and upper floors was performed by specialists from Ras Group Project LLC using the Lira SAPR-2022 software package. A general view of the adopted finite element 3D model of the building is shown in **Figure 5**.

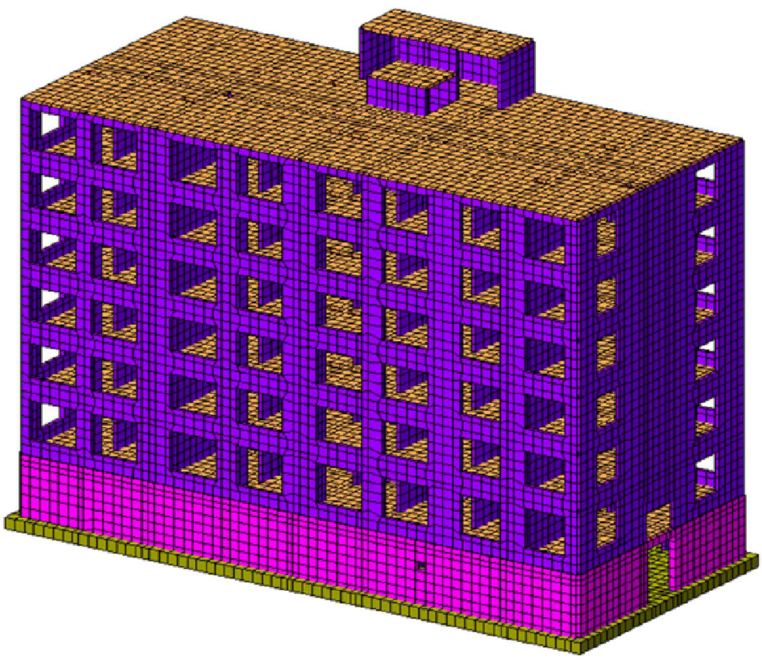

Figure 5. Calculation model of a 6-story building.

Summary of the performance of the control structural analysis and the results of the calculated estimates used in compiling this document are provided below.

For the determination of the design horizontal seismic force F_{ik} using the spectral method, the following expression should be used:

$$F_{ik} = \gamma_{Ih} \cdot S_d(T_i) \cdot m_{ik} \tag{1}$$

where

F_{ik} is the seismic load on the structure in the considered horizontal direction for the *i*-th mode of its natural vibrations, applied to point *k*;

γ_{Ih} is a coefficient taking into account the combination of responsibility classes and used to determine the effects of horizontal seismic impacts; it should be taken in accordance with Table 7.4 of SP RK 2.03-30-2017* for all structures and equal to at least $\gamma_{Ih} = 1.06$ (see also subsection 4.3 of these STS);

$S_d(T_i)$ is the value of the design response spectrum in accelerations over the period T_i;

T_i is the period of structure vibrations for the *i*-th mode in the considered horizontal direction;

m_{ik} is the effective modal mass, referred to point *k*, corresponding to the *i*-th vibration mode, determined using the expression:

$$m_{ik} = m_k \cdot \eta_{ik} \tag{2}$$

where

η_{ik} is a coefficient depending on the structure's deformation mode during its natural vibrations at the *i*-th tone, the load location, and the direction of the seismic impact.

Design response spectra:

The horizontal seismic impact is described by two orthogonal components, considered independent and characterized by identical response spectra.

For the horizontal components of the seismic impact taken into account in the design of each of the buildings under consideration, the design response spectrum $S_d(T)$ is determined using the following expressions:

$$\begin{gathered} 0 \leq T \leq T_C : \\ S_d(T) = a_g \cdot \frac{2.5}{q} \end{gathered} \tag{3}$$

$$\begin{gathered} T \geq T_C : \\ S_d(T) = a_g \cdot \frac{2.5}{q} \cdot \frac{T_C}{T}, \quad \text{but not less than } \beta a_g \end{gathered} \tag{4}$$

where

$S_d(T)$ is the design response spectrum characterizing the horizontal component of the seismic impact;

T_C is the maximum period on the constant section of the spectral acceleration graph, which should be taken as 0.96 s corresponding to soil condition type third (IIIrd);

T is the period of vibration of a linear system with one degree of freedom in the horizontal direction;

a_g is the calculated horizontal acceleration at the construction site, which should be taken as $a_g = 0.66g$ (see subsection D.1);

β is the lower limit of the spectrum of calculated responses for horizontal components, taken as 0.2 (see 7.5.2 of SP RK 2.03-30-2017*);

q are the behavior coefficients taken into account when determining the design horizontal seismic loads, the values of which, subject only to the regularity criteria in plan and height regulated in Appendix G to SP RK 2.03-30-2017*, should be taken as for wall structural systems (taking into account the manifestation of the ability of structural elements to undergo plastic deformation) according to 7.6.1, Table 7.8 of SP RK 2.03-30-2017*, equal to:

- $q_x = q_y = 4.0$ in the longitudinal principal X-direction; in the transverse principal Y-direction.
- Responsibility class by number of storeys: third (IIIrd)—high-rise building.
- Responsibility class by functional purpose: second (IInd).

Note: The behaviour factor q is an approximate value of the ratio of the seismic loads that would act on a building or structure with its fully elastic response and viscous damping of 5% to the seismic loads that may be used in a design based on the results of a linear elastic analysis.

For the vertical component of seismic impacts taken into account in the design of each of the buildings under consideration, the design response spectrum $S_{dv}(T)$ is determined using the following expressions:

$$\begin{gathered} 0 \leq T_v \leq T_{Cv}: \\ S_{dv}(T) = a_{gv} \cdot \frac{2.25}{q} \end{gathered} \tag{5}$$

$$\begin{gathered} T_{Cv} \leq T_v \leq 2.0: \\ S_{dv}(T) = a_{gv} \cdot \frac{2.25}{q} \cdot \left[\frac{T_{Cv}}{T_v}\right]^k \end{gathered} \tag{6}$$

Where:

$S_{dv}(T)$ is the design response spectrum characterizing the vertical component of the seismic impact;

T_{Cv} is the maximum value of the period on the constant section of the spectral acceleration graph, taken to be 0.2 s;

T_v is the period of vibration of a linear system with one degree of freedom in the vertical direction;

a_{gv} is the calculated vertical acceleration at the construction site, which should be taken as a_{gv} = 0.59g (see the report of KazGIIZ LLP);

k is the exponent, which should be taken as corresponding to the third type of soil conditions (IIIrd) and equal to 0.35 (see Table 7.6 of SP RK 2.03-30-2017*, the report of KazGIIZ LLP, as well as 7.4.1, 7.4.2 of SP RK 2.03-31-2020 [21]);

q is the behavior coefficient taken into account when determining the calculated vertical seismic loads; for all the structures under consideration, $q = 1.5$ should be taken (see also 7.6.2 of SP RK 2.03-30-2017*).

2.5. Technical condition of the test object

At the initial stage of the preparatory work associated with the vibro-dynamic testing program, a condition assessment of the full-scale test object was carried out and its technical condition was evaluated.

The inspection included a visual check of the conformity of the actual structural solutions with the design and photographic documentation of any identified discrepancies and/or structural defects.

The building's plan dimensions at the outer axes are 12.8 × 29.0 m.

At the time of testing, the representative building included a basement and 6 above-ground floors. The height of the section from ground level to the top of the roof slab was 22.2 m.

According to the inspection results of the representative building, the following was established:

- Concrete overflows were detected at the junctions of vertical structures with the floor and roof slabs, see **Figure 6**;
- In the corners of window and door openings, in some places there are minor hairline cracks with an opening width of less than 0.05 mm, see **Figure 7**;
- Minor concrete spalling and process cracks were detected in the vertical wall structures, see **Figure 8**.

Overall, the technical condition of the full-scale object prior to the start of the vibro-dynamic testing can be assessed as satisfactory.

Figure 6. Concrete sag at the floor and roof level.

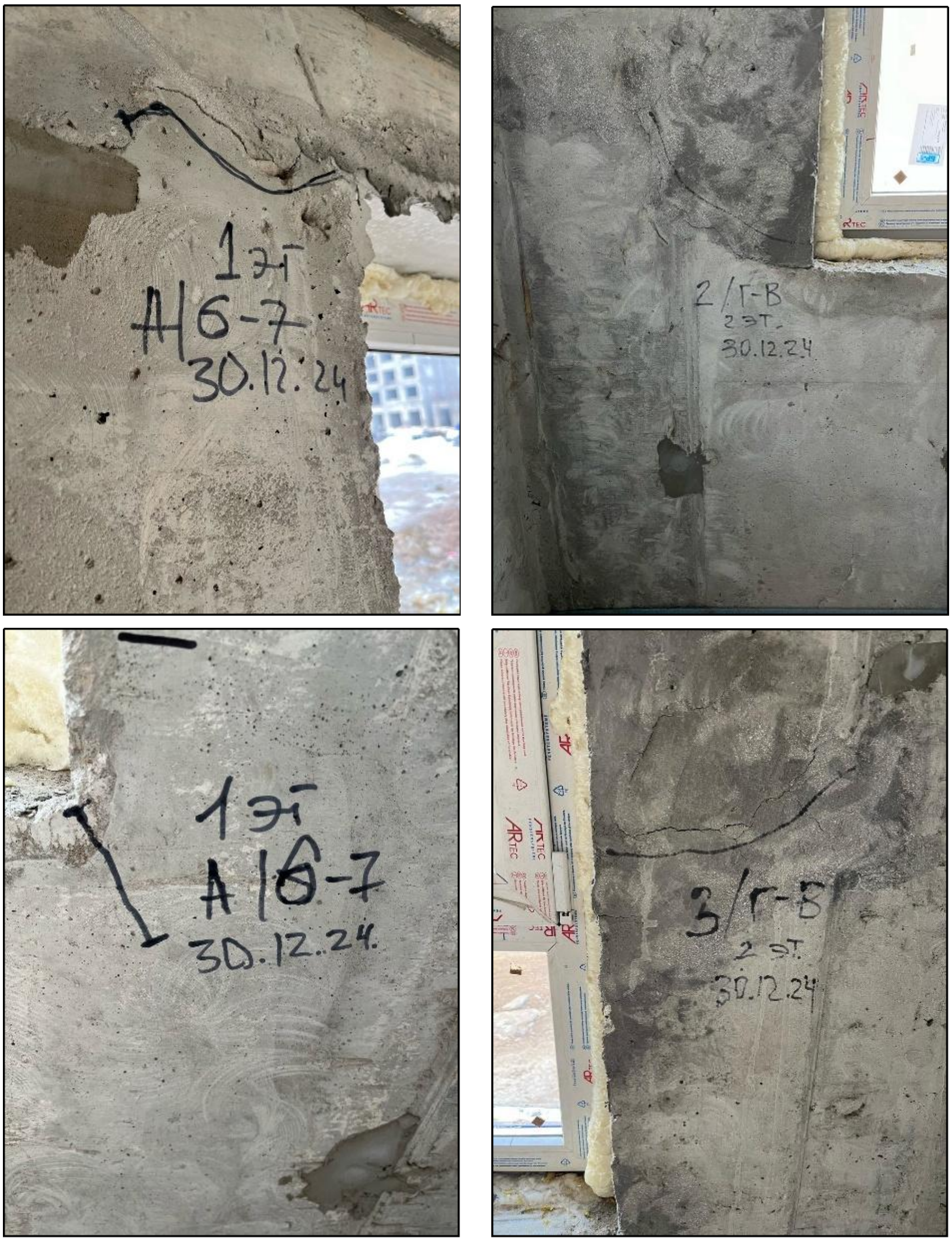

Figure 7. Hairline cracks with an opening width of up to 0.05 mm in door and window openings.

Figure 8. *Cont.*

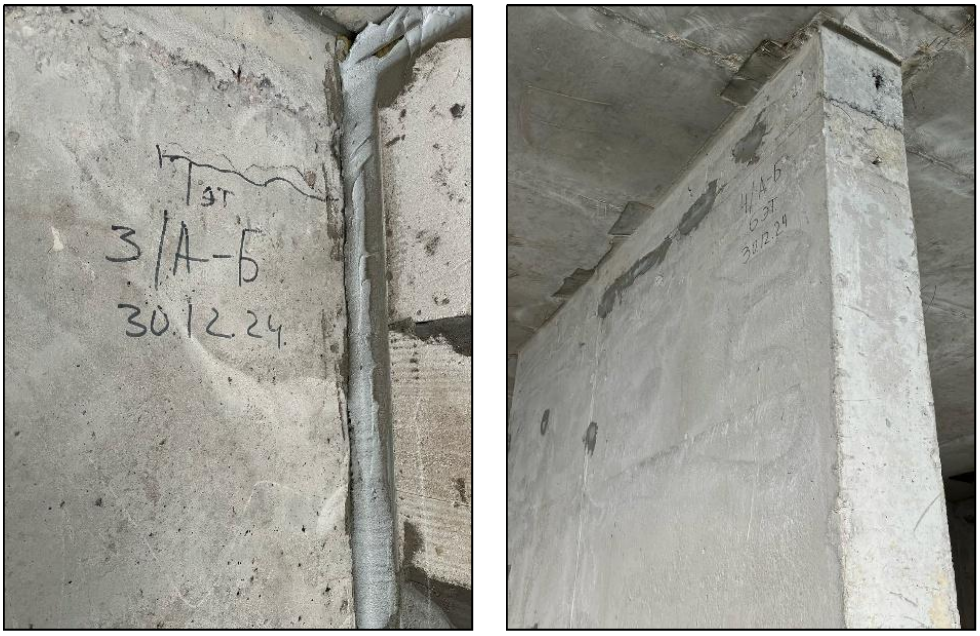

Figure 8. Concrete spalling at the floor and roof level, and process cracks in vertical structures.

2.6. Brief information on the equipment

In the experimental studies carried out, dynamic loads on the object under study were created using a B-3 type inertial vibration machine.

B-3 type vibration machines are among the most powerful in the world. They can develop a shaft excitation force of 50–15,000 kN (depending on the number of connected vibrators, the loads attached to the vibrators, and the rotational speed of the vibrator arms).

Dozens of full-scale objects have been tested using B-3 type vibration machines in the Republic of Kazakhstan and other CIS countries. The results obtained in these tests have been repeatedly confirmed by analysis of the effects of strong earthquakes.

The power equipment set for vibration testing of the building included:

- A 200 kW DC motor;
- Five twin-shaft vibrators with horizontal axes of rotation of the eccentric weight levers;
- Additional eccentric weights, attached to the vibrator levers if necessary;
- A control panel allowing smooth adjustment of the motor shaft speed.

During testing, the motor and vibrators were rigidly attached to a horizontal steel frame located at the building's roof level. The steel frame was rigidly attached to this roof.

The layout of the vibration machine on the building's floor is shown in **Figure 9**. From **Figure 9**, it can be seen that the adopted layout of the vibration machine allowed for the excitation of building vibrations in the intended direction of one of its main orthogonal axes of inertia in the transverse direction of the building.

Figure 9. Inertia-type vibrating machine.

3. Results

3.1. Brief information on the test procedure

The vibration tests conducted on the object included VI stages, each of which (from stage I to stage V) was characterized by increasing the applied forces generated by the inertial vibration machine (B-3 type vibration machine). The number of connected vibrators and the number of eccentric masses on the vibration machine arms increased from stage I to stage V; in stage VI, the number of eccentric masses was reduced. The quantitative characteristics of the test stages are presented in **Table 1**.

Table 1. Quantitative characteristics of the test stages.

Test stage number	Number of interlocked vibrators	Number of eccentric weights on all vibrators
I	1	0
II	5	0
III	5	100
IV	5	200
V	5	300
VI	5	160

Each test stage consisted of a double, smooth passage through resonances: first by increasing the rotational speed of the vibration machine shafts equipped with unbalanced levers (direct resonance), and then by decreasing the frequency (reverse resonance).

At each stage of testing, the following was carried out: instrumental recording of the building vibration amplitudes and prompt processing of the measurement results; real-time visual inspection of the structures and photographic recording of their condition; and video recording of the structure's behavior under dynamic loads.

Final processing and analysis of experimental data were carried out in laboratory conditions. Instrumental data were recorded using a dedicated hardware and software system.

The hardware consists of an analog signal input unit with an analog-to-digital conversion device, connected to a PC-based signal recording and processing unit. A general view of the hardware and software system during operation and the sensors is shown in **Figures 10** and **11**.

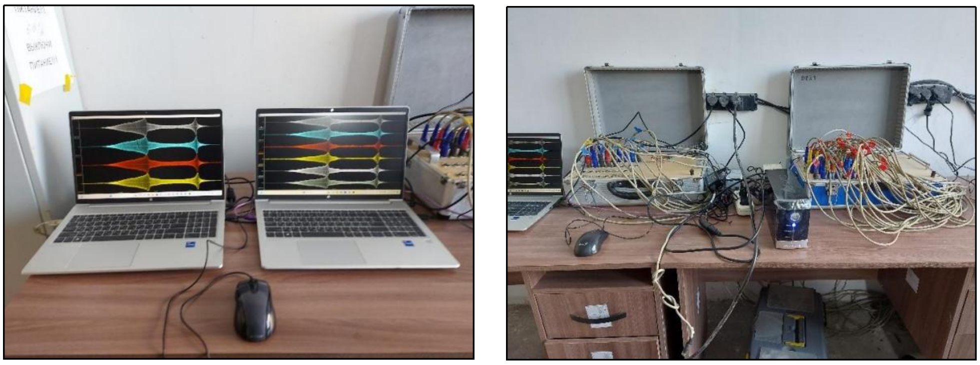

Figure 10. General views of recording systems.

Figure 11. General views of sensors.

A total of 38 accelerometer sensors were used in the tests.

The PCM-32 digital measurement system was used. The sampling frequency range was 0.61–625 Hz; a frequency of 156.25 Hz was adopted for the tests, corresponding to an accelerogram digitization time step of 0.0064 s. The accelerometers had an acceleration measurement range of 0 to 4g. The electrical signals from the accelerometer outputs were converted by the digital system into a sequence of digital signals and then recalculated into acceleration values. Conventional accelerograms were obtained, from which peak acceleration values were subsequently extracted; the signals were passed through digital filters, etc.

The adopted sensor arrangement allowed for recording:

- Spatial patterns of building vibrations;
- Deformations of interfloor slabs due to their compliance;
- Horizontal and vertical deformations of the building foundation;
- Distortions of floors.

3.2. Initial dynamic parameters of the test object

The initial dynamic parameters of the experimental object were determined from instrumental recordings of its microseismic vibrations caused by the impact of the load on the roof (see **Figure 12**).

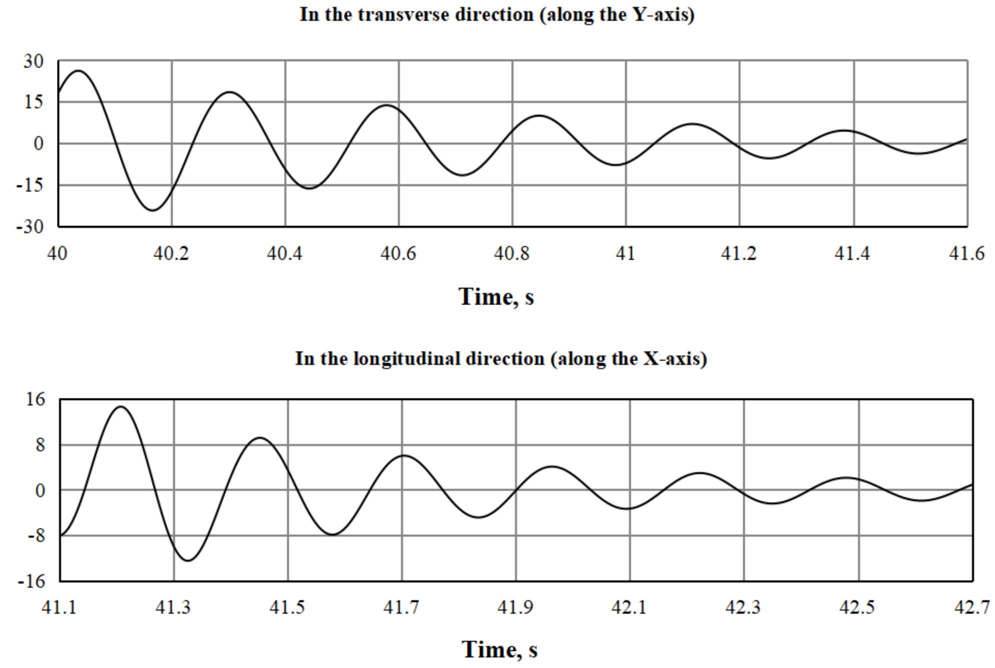

Figure 12. Instrumental recordings of microseismic vibrations of the building.

From the obtained instrumental recordings, it follows that before the start of the tests, the period of free damped vibrations of the object in the first mode in the transverse direction (along the Y-axis) was 0.272 s, and in the longitudinal direction (along the X-axis)—0.253 s.

The logarithmic decrements of the experimental object vibrations had the following values: in the transverse direction—approximately 0.35–0.37, in the longitudinal direction—approximately 0.37–0.39.

3.3. Horizontal loads impacting on the test object

The maximum horizontal loads impacting on the test object during its fundamental vibrations in the transverse direction at different test stages are presented in **Table 2**. The loads on the test object, listed in **Table 2**, were determined based on the actual mass of the object.

Table 2. Values of horizontal loads.

Floor elevation by object height	Values of horizontal loads impacting on the object in the transverse (Y) direction during the testing stages, tf					
	I	II	III	IV	V	VI
18.500	15.65	62.06	136.74	188.34	230.45	173.31
15.300	13.31	53.20	117.48	161.62	197.24	148.35
12.300	11.43	45.45	100.16	138.12	168.11	126.02
9.300	9.16	36.71	82.33	113.65	138.48	103.05
6.300	6.81	27.85	63.86	88.39	107.87	79.59
3.300	4.88	20.05	47.03	64.98	79.07	57.44
0.000	3.03	13.22	32.62	45.26	54.34	38.59
−3.600	2.25	10.83	27.64	37.65	44.71	31.50
Total	66.53	269.36	607.87	838.01	1,020.26	757.85

Table 2 shows that the maximum horizontal loads impacting on the test object during its fundamental vibrations in the transverse direction at test stage V were 1,020.26 tf.

3.4. Vibration mode coefficients of the test object

The values of the vibration mode coefficients, depending on the deformation modes of the object during its vibrations, were determined using the formula:

$$\eta_{ik} = \frac{X_i(x_k)\sum_{j=1}^{n} Q_j X_i(x_j)}{\sum_{j=1}^{n} Q_j X_i^2(x_j)} \tag{7}$$

where

$X_i(x_k)$ and $X_i(x_j)$ are the displacements of the building during natural vibrations at the *i*-th tone at the point *k* under consideration and at points *j* where the masses are concentrated;

Q_j is the weight of the concentrated mass referred to point *j*;

n is the total number of concentrated masses.

The calculated values of the object's vibration mode coefficients for the fundamental tone in the transverse direction are presented in **Table 3**.

Table 3. Vibration mode factors of the object.

Marking an object by height	The vibration mode coefficients of an object for the fundamental (first) tone in the transverse direction at the test stages					
	I	II	III	IV	V	VI
18.500	1.415	1.429	1.435	1.433	1.435	1.433
15.300	1.239	1.264	1.271	1.269	1.265	1.266
12.300	1.116	1.078	1.080	1.083	1.079	1.074
9.300	0.812	0.878	0.889	0.892	0.888	0.878
6.300	0.639	0.664	0.692	0.696	0.693	0.680
3.300	0.417	0.463	0.498	0.499	0.495	0.481
0.000	0.228	0.262	0.300	0.306	0.298	0.283
−3.600	0.107	0.136	0.152	0.151	0.145	0.136

3.5. Influence of foundation flexibility on building displacement

To assess the influence of the foundation flexibility on the displacement values of the test object, instrumental records obtained at the level of its roof and at the level of the foundation slab were analyzed.

This analysis resulted in the determination of the proportions of test object displacement at the roof level during its translational vibrations due to:

- Foundation flexibility in shear;
- Foundation flexibility in rotation;
- Flexibility of the structural system ("box") of the object.

The analysis results are presented in **Table 4**.

The deformation pattern of the transverse wall of the object along axis 1, illustrating the effect of foundation compliance on building displacement, is shown in **Figure 13**.

Table 4. Evaluation of the influence of foundation compliance on the displacement values of the test object.

Test stage number	Displacement of the center of the test object's roof (mm)	Roof displacement due to foundation shear (%)	Roof displacement due to foundation rotation (%)	Roof displacement due to structural-system deformation (%)
I	0.690	7.542	43.402	49.056
II	3.192	9.541	49.443	41.016
III	9.441	10.56	58.82	30.62
IV	15.279	10.554	59.148	30.298
V	21.676	10.108	59.291	30.601
VI	14.428	9.52	54.925	35.555

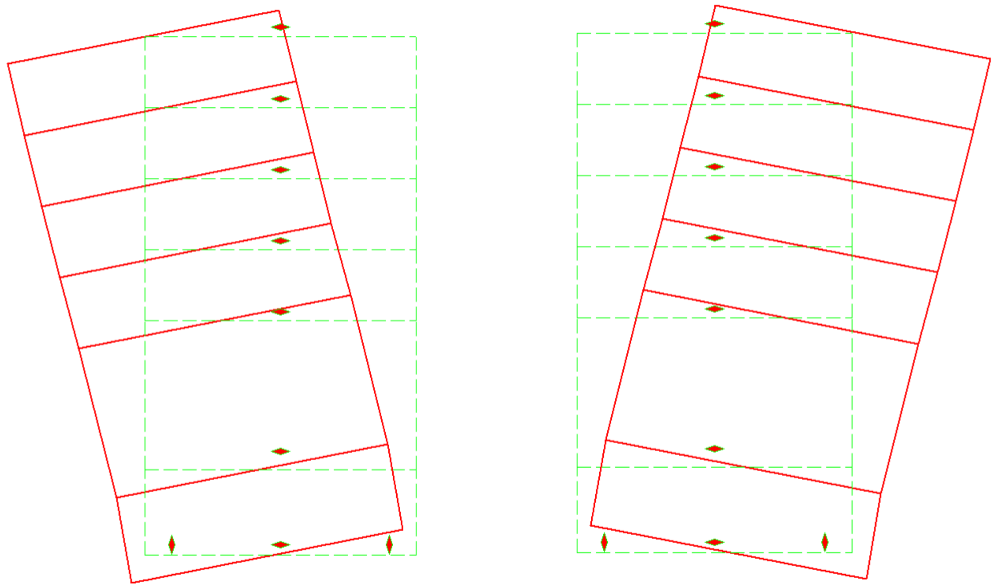

Figure 13. Deformation pattern of the transverse wall of the object along axis 1.

3.6. Results of a visual inspection of load-bearing and non-load-bearing structures after vibration exposure

The results of a visual inspection of the building's load-bearing and non-load-bearing structures after vibration exposure showed the following.

There was no significant damage to the supporting structures of the experimental object after all stages of vibration exposure. Only in individual load-bearing walls and lintels were hairline cracks of varying lengths observed, developing from the corners of window and door openings, and minor openings of existing cracks of a technological nature in the walls (see **Figure 14**).

In separate non-load-bearing structures (partitions) and in places where they adjoin adjacent structures, the formation of cracks, partial crumbling of cement-sand mortar at the floor level, and partial damage to the stonework and chips (aerated concrete blocks) were visually noted (see **Figure 15**).

The superstructure on the roof, made of masonry, partially collapsed.

According to the provisions of SN RK (Construction Standards of the Republic of Kazakhstan) 2.03-28-2004 "MSK-64(K) Scale for Earthquake Intensity Assessment," the damage to most load-bearing building structures can be rated as "0" (no visible damage), with only a few structures receiving a "1" (barely noticeable cracks).

Figure 14. Small hairline cracks developing from the corners of window openings after stage II.

Figure 15. Damage to partitions at the junctions with the floor.

Damage to non-load-bearing structures in most cases can be rated as "0" (no visible damage) and only in a few cases was it close to "1"—cracks in individual non-load-bearing partitions (up to 3%) and their connections with load-bearing elements, crumbling pieces of plaster and mortar at the points of contact with floor slabs and load-bearing walls.

When assessing the extent of damage to load-bearing and non-load-bearing structures, it should be taken into account that during the vibration exposure process, the building underwent 6 stages of testing, during which it completed approximately several hundred vibration cycles with accelerations of 0.1–0.532g. In other words, non-load-bearing structures were subjected to alternating horizontal loads several hundred times.

Under actual seismic impacts, the number of vibration cycles for a building of this type (in the worst case) would be no more than 100–150.

Overall, the building's condition after vibration testing is fully consistent with the condition stipulated by the scientific and methodological principles of the current regulations "Construction in Seismic Zones".

3.7. Recommendations for strengthening building structures with identified defects

Based on the results of a visual inspection before and after vibrodynamic testing, specialists from KazNIISA JSC did not identify any significant damage requiring strengthening. However, the following actions are required:

a) All cracks that have appeared and are present during all stages of testing must be cleaned and then grouted.

b) All unevenness on the surface and at the corners of the concrete should be leveled with a cement-sand mortar of at least grade M200.

c) Gaps that have formed where partitions meet load-bearing structures must be cleaned and then sealed.

d) Damaged masonry of superstructures on the roof must be dismantled and subsequently restored.

e) Non-load-bearing enclosing walls must be constructed of hollow concrete blocks. The masonry of non-load-bearing walls must be reinforced in accordance with the results of their calculations for local seismic loads. The design of non-load-bearing walls made of hollow concrete blocks must comply with the provisions of the Technical Solutions "Enclosure Structures of Individual Residential Buildings Constructed in Seismic Regions Using Efficient Building Materials. Part 5: Non-Load-Bearing and Self-Supporting Walls of Hollow Concrete Blocks" published by KazNIISA (Kazakhstan Research and Design Institute of Construction and Architecture) RSE, Almaty, 2005.

4. Analysis of instrumental data obtained during vibration testing of the experimental object

4.1. Comparison of calculated and experimental values of the experimental object's vibration periods

The calculated and experimental values of the experimental object's vibration periods are presented in **Table 5**.

Table 5. Calculated and experimental values of the experimental object's vibration periods.

Building vibration modes	Building vibration period values, s		
	Microseismic	Experimental	Calculated
First translational along the X-axis	0.253	–	0.271/0.333
First translational along the Y-axis	0.272	0.277/0.405	0.429/0.568

Note: The experimental values of the vibration periods given in the numerator correspond to the initial stages of testing, and those in the denominator correspond to stage V of testing. The calculated values of the vibration periods given in the numerator are determined in accordance with D.5 of SP RK 2.03-30-2017* with the equivalent foundation rigidity increased by 1.5 times, and those in the denominator are decreased by 1.5 times.

The following explanation should be added to the note. The regulatory document contains a set of rules of the Republic of Kazakhstan 2.03-30-2017* [25]. There is an Appendix D, which regulates the determination of the stiffness of the base in case there are no results of measuring the velocity of the elastic wave at the construction site. In this case, two dynamic models of the foundation are considered. In one case, the equivalent stiffness of the base increases by 1.5 times, and in the other it decreases by 1.5 times (paragraph D.5.1). Therefore, there is a semi-empirical way to determine the estimated oscillation period. As a result, the calculation results in two values of the oscillation period. In fact, the range of values of the oscillation period is obtained, within which the true oscillation period is located. This explains the discrepancy between the experimental and calculated oscillation periods.

The following conclusions can be drawn from the data in **Table 5**:

a) The resonant periods of the building's vibrations depended on the level of the loads impacting on it. The values of the resonant periods of the building's vibrations in the transverse direction (along the Y-axis) during the final stages of testing exceeded the values of the initial periods by 1.462 times;
b) The change in the resonant periods of the building's vibrations as the intensity of external vibration influences increased can be explained by the nonlinear behavior of the building's foundation and supporting structures;
c) The periods of the building's vibrations during microseismic recordings differed from the calculated values:

    - For the fundamental tone in the longitudinal direction (along the X-axis)—by 1.07/1.32 times;
    - For the fundamental tone in the transverse direction (along the Y-axis)—by 1.58/2.09 times.

The period of vibrations of the building at the fundamental tone during microseismic vibrations in the longitudinal direction (along the X-axis) was close to the calculated values with the equivalent rigidity of the foundation increased by 1.5 times.

d) The experimental values of the building's vibration periods at stage I of testing differed from the calculated values:

    - For the fundamental tone in the transverse direction (along the Y-axis)—by 1.55/2.05 times.

The experimental values of the building's vibration periods at stage V of testing differed from the calculated values:

- For the fundamental tone in the transverse direction (along the Y-axis)—by 1.06/1.4 times.

The periods of vibration of the building along the fundamental tone at stage V of testing in the transverse direction (along the Y-axis) were close to the calculated ones with the equivalent rigidity of the foundation increased by 1.5 times.

Differences between the calculated and experimental vibration periods of the test object do not affect the seismic loads assumed in the building design, since all period values fall within the straight section of the response spectrum, which extends up to a period of $T_c = 0.96$ s.

4.2. Effects of nonlinear deformation of the test object under vibration

Figure 16 shows the load-displacement dependencies characterizing the degree of nonlinear deformation of the test object-foundation system (**Figure 16a**) and the test object's structural system (**Figure 16b**) (without the influence of the foundation's flexibility) under vibration impacts in the transverse direction of the building (along the Y-axis).

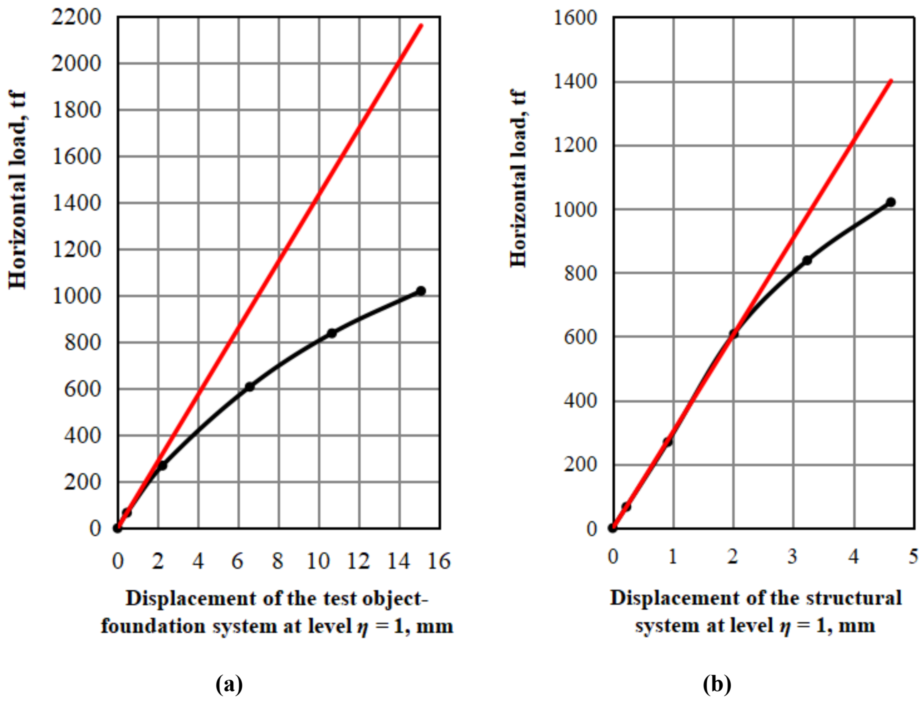

Figure 16. Load-displacement relationships characterizing the degree of nonlinear deformation of: **(a)** The test object-foundation system; **(b)** The test object's structural system in the transverse direction.

Note: From here on, level $\eta = 1$ refers to the height of the test object at which the vibration shape factor η has a value of 1.0.

In **Figure 16**, the black lines show the load-displacement relationships constructed based on experimental data, while the red lines represent the relationships characterizing the actual initial stiffnesses of the system. **Figure 16a** shows that the constructed relationship has a pronounced nonlinear nature. **Figure 16b** shows that the structural system of the test object began to exhibit nonlinear behavior at loads of approximately 600 tf.

At maximum loads, the stiffness of the test object-foundation system decreased by 2.14 times compared to the initial stiffness, while the stiffness of the test object's structural system decreased by 1.37 times.

The obtained data indicate that the nonlinear nature of the deformation of the test object was caused mainly by the nonlinear operation of the soil base and, to a lesser extent, by the structural system.

Conclusions regarding the degree of reduction in the initial stiffness of the test object under vibration impact can also be drawn from the results of comparing the resonant vibration periods of the test object at the initial and final stages of testing.

The dependence characterizing the values of the resonant periods of vibrations of an object at different amplitudes of its vibrations is shown in **Figure 17**.

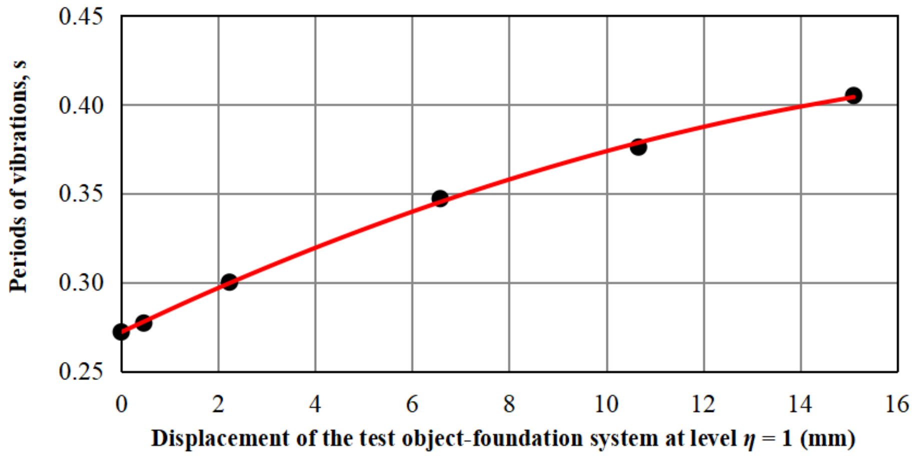

Figure 17. The vibration periods-displacements relationship characterizing the degree of nonlinear deformation of the test object-foundation system.

The ratios between the vibration periods of the object at the initial and final stages of testing are: 0.405/0.277 = 1.462.

From this relationship, it follows that, under maximum loads, the stiffness of the test object-foundation system decreased by a factor of 2.14 compared to the initial stiffness.

From the above data, it follows that the estimates of the reduction in the initial stiffness of the test object-foundation system obtained by different methods are virtually identical. This demonstrates the reliability of the obtained instrumental data.

4.3. Comparison of calculated and experimental loads impacting on the test object

A comparison of the quantitative characteristics of the calculated seismic loads on the designed building and the dynamic loads impacting on the object during testing in the transverse direction is given in **Table 6**. The calculated values of the horizontal seismic loads in **Table 6** for the experimental object were determined based on its actual vibration periods and the actual mass of the object at the time of testing.

Table 6. Experimental and calculated values of horizontal loads.

Calculated loads, tf	Experimental values of horizontal loads impacting on the building during testing, tf					
	I	II	III	IV	V	VI
1,203.35 (100%)	66.53 (5.53%)	269.36 (22.38%)	607.87 (50.51%)	838.01 (69.64%)	1,020.26 (84.78%)	757.85 (62.97%)

Table 6 shows that the maximum horizontal inertial forces impacting on the experimental object during testing (taking into account the fact that some of the loads acting on the object during operation were absent during the testing period) amounted to 84.78% of the calculated 10-point loads.

It should also be noted that a characteristic feature of vibration testing is the non-stationary passage of the test objects through resonances. During non-stationary passage through resonances, the corresponding maximum vibration amplitude of the test object is not achieved, and, as a result, its dissipative properties are overestimated.

4.4. Dissipative properties of the test object

The dissipative properties of the test object interacting with the ground base during vibration were assessed using dynamic coefficients.

The dynamic coefficient values for each test stage were determined using the following formula:

$$K_d = \frac{M \cdot A_{\eta=1}}{(mr)_v \cdot \eta_v} \tag{8}$$

where

$A_{\eta=1}$ is the resonant amplitude of the object's vibrations at the point with the vibration shape factor $\eta = 1$;

$(mr)_v$ is the moment of the vibration machine's eccentric weight;

η_v is the vibration shape factor of the building at the vibration machine's installation location;

M is the reduced mass of the test object, determined using the following formula:

$$M = \sum_{k=1}^{n} m_k \cdot \eta_k^2 \tag{9}$$

where

η_k is the vibration shape factor of the object at point *k*;

m_k is the mass of the test object, concentrated at point *k*.

When structures operate in the elastic phase, a relationship exists between the values of the dynamic coefficients and the logarithmic decrements of vibration:

$$\delta = \frac{\pi}{K_d} \tag{10}$$

When structures operate nonlinearly, this relationship does not strictly reflect the actual characteristics of energy dissipation by the system and can only be used to approximately estimate the dissipative properties of a conventional linear oscillator simulating the test object.

The calculated logarithmic decrements of vibration of the test object in the transverse direction of the building are presented in **Table 7**.

Table 7. Logarithmic decrements of vibration in the transverse direction of the building at test stages.

I	II	III	IV	V	VI
0.462	0.457	0.458	0.458	0.459	0.458

Table 7 shows that the change in the logarithmic decrements of vibration at different test stages was insignificant.

Note that the definition of the logarithmic decrement is based on a simplified linear formula. However, this is due to the fact that the building received minimal damage during dynamic tests—small hairline cracks in the area of the window openings (**Figure 14**) and damage to the partitions at the junction with the ceiling (**Figure 15**). There is no reason to believe that these damages significantly changed the dissipative properties of the building. The analysis of the consequences of strong earthquakes is always associated with significant damage to the supporting structures of the building. This includes the appearance of through cracks in load-bearing structures with a large opening width, the appearance of plastic hinges, etc. There were no such effects in these experimental studies. In Section 4.7, the reliability calculation will be performed with various dissipative characteristics.

4.5. Non-linearity coefficients

The ability of the test object under consideration for nonlinear operation can be estimated using the nonlinearity coefficient μ.

The values of the coefficient μ can be determined using the following formula:

$$\mu = (T_{\text{res}}/T_{\text{init}})^2 \tag{11}$$

The values of the coefficients μ calculated for different test stages in the transverse direction of the building are presented in **Table 8**.

Table 8. Values of non-linearity coefficients.

Test stage	Vibration period	Coefficient of nonlinearity μ
Before Testing	0.272	1.000
I	0.277	1.037
II	0.300	1.216
III	0.347	1.628
IV	0.376	1.911
V	0.405	2.217
VI	0.381	1.962

The relatively small values of the coefficient μ corresponding to test stages III–VI indicate significant reserves of the test object's ability to develop plastic deformations. The test object is a monolithic building with a very substantial reserve of load-bearing capacity.

4.6. Criteria for the regularity of a building in plan and height

The maximum and average horizontal displacements of the extreme points of the building's slabs for the primary first translational vibration mode in the transverse direction did not exceed 2.1%.

For all adjacent floors of the building, except the top floor, the following condition is met (see **Table 9**):

$$\frac{d_{e,k} \cdot h_{k+1}}{d_{e,k+1} \cdot h_k} \leq 1.25 \quad (12)$$

where

$d_{e,k}$ and $d_{e,k+1}$ are the differences in the average horizontal displacements of the upper and lower floors of floor k and floor $k+1$, respectively;

h_k and h_{k+1} are the heights of floors k and $k+1$.

Table 9. Building regularity condition in the transverse direction at stage V of testing.

Floor	h_k, m	$d_{e,k}$, mm	$\frac{d_{e,k} \cdot h_{k+1}}{d_{e,k+1} \cdot h_k} \leq 1.25$
6	3.0		
5	3.0	2.875	1.021
3	3.0	2.950	1.026
3	3.0	2.985	1.012
2	3.0	2.979	0.998
1	3.3	2.315	0.706
−1	3.6	2.191	0.868

Based on the test results, the building is classified as regular in plan and regular in height.

4.7. Building reliability calculation

Building reliability is defined as the probability of its failure-free operation.

Reliability W is the probability of failure-free operation: $W = W(|y| < [h])$, where y is the coordinate along the transverse axis of the building, and h is the building's height, equal to 22.2 m and equal to $[h]$ = 5.55 cm. This corresponds to $[h] = h/400$, which is typical for buildings constructed from monolithic wall structures [17].

To calculate reliability, instrumental data from the engineering and seismometric service of KazNIISA JSC and seismic stations of the Institute of Seismology (now the National Scientific Center for Seismological Observations and Research of the Ministry of Emergency Situations of the Republic of Kazakhstan) are used. This allows for consideration of the regional characteristics of seismic impact in the Northern Tien Shan region.

In general, for the analysis of the reaction and for the assessment of the reliability of monolithic buildings, a single-mass cantilever system with a concentrated mass and a nonlinear deformation diagram (DD) can serve as an acceptable calculation model. The following nonlinear differential equation is integrated in the general case:

$$m\ddot{y} + \beta\dot{y} + R(y) = -m\ddot{y}_{0i} \quad (13)$$

where:

$R(y)$ is the experimental nonlinear restoring force (deformation diagram);

$\ddot{y}_{0i}$ is the i-th accelerogram;

β is the coefficient of viscous friction (Voigt's hypothesis), adopted based on experimental data;

m is the mass of the construction object (building), $m = Q/g$, g is the acceleration due to gravity,

y is the horizontal displacement.

In the calculations, $Q = 981T$, $\beta = 10T$·c/sm.

The deformation diagram is approximated by a piecewise linear dependence and is shown in **Figure 16a**.

The seismic impact on the right-hand side of Equation (13) was modeled by a non-stationary random process, which is obtained by multiplying the realizations of a normal stationary process by a deterministic envelope in the form of F.F. Aptikaev. The envelope takes into account the regional characteristics of seismic impact for the Almaty region [26].

The correlation function of a normal stationary random process is adopted as

$$K(\tau) = \sigma^2 e^{-\alpha|\tau|} \left[\cos(\omega\tau) + \frac{\alpha}{\omega}\sin(\omega|\tau|)\right] \tag{14}$$

where α is the correlation parameter, ω is the carrier frequency of the impact, and σ is the acceleration standard at the base of the calculation model.

The acceleration value of 0.66g is the peak ground acceleration (PGA). It was adopted on the basis of the Seismic Zoning Map of the Territory of Almaty. When accelerograms are generated to calculate reliability—the probability of failure-free performance—using the Monte Carlo method, the sample mean for, for example, a sample of 1,000 accelerograms is approximately equal to the specified value.

The parameters of correlation Equation (14) were adopted using regional seismological data from the National Scientific Center for Seismological Observations and Research of the Ministry of Emergency Situations of the Republic of Kazakhstan. The value of β was adopted as β = 23.25 s^{-1}. In essence, this value is equal to the carrier frequency of the seismic action, which was obtained by analyzing the vibration frequencies of the ground at the free surface. The value of α is α = 11.63 s^{-1} and was obtained on the basis of instrumental records (accelerograms) of the 1990 Baysorun earthquake and the earthquake of March 4, 2024.

Reliability calculations for W are performed using statistical testing (the Monte Carlo method) using the SCILAB computer mathematics system. A standard scheme was used: sequentially, using a shaping filter method, realizations of a random process with the above correlation function and a specified envelope are generated [26]. The root-mean-square acceleration values were selected to ensure that the average acceleration value coincided with the 0.66g acceleration value from Section 2.4. Statistical characteristics of the response parameters are obtained by processing the resulting set using standard methods of mathematical statistics.

Nonlinear differential Equation (13) is integrated numerically using a combination of the multi-step Adams method and the rarely used inverse differentiation method. For each realization, the kinematic parameters of the building model are determined, and the failure criterion is verified. Special modules were written to perform the calculations. This combination of methods integrates nonlinear differential equations with sufficient accuracy.

Table 10 shows the results of calculating the probability characteristics (mean and standard deviation) of the displacement and speed of the system, the reliability values W and failure Q. 1,000 realizations of the random process (artificial accelerograms) were generated. The average acceleration at the base is almost identical to the value of 0.66 g from Section 2.4.

Table 10. Probabilistic characteristics of the building response at different average acceleration values, cm/s^2.

Parameter	657.53	347.83	148.53
Average displacement, cm	5.084	2.493	0.931
Displacement standard, cm	0.749	0.419	0.143
Average velocity, cm/s	32.014	32.014	12.885
Velocity standard, cm/s	12.041	6.84	2.904
Reliability value W	0.735	1.0	1.0
Failure value Q	0.265	0.0	0.0

The analysis shows that the reliability value W is quite high. According to regulatory documents, the building's service life is 50 years. The acceleration values are based on a recurrence map of 1 seismic event in 475 years. Therefore, the probability of a seismic event is 0.1053. Therefore, $Q_{475} = 0.265 \times 0.1053 = 0.02789$. Then, the reliability $W_{475} = 1 - 0.02789 = 0.972$. This value is quite high.

For impacts of lower intensity from **Table 11**, the failure probability $Q = 0$. To assess the accuracy of determining reliability values and the probabilistic characteristics of the response parameters, these values were determined using different numbers of artificial accelerograms (realizations of a random process with correlation Equation (14) used in the statistical testing method. Analysis of **Table 11** shows that, as the number of realizations increases, both the reliability values and the probabilistic characteristics of the response parameters converge.

Table 11. Probabilistic characteristics of the response of a 6-story building with a different number of implementations.

Parameter	100	500	1,000	2,000	3,000	4,000
Average displacement, cm	5.13	5.067	5.084	5.078	5.132	5.114
Displacement standard, cm	0.78	0.743	0.749	0.744	0.785	0.771
Average velocity, cm/s	54.86	53.851	53.901	54.104	54.78	54.540
Velocity standard, cm/s	12.29	11.61	12.041	11	12.27	12.08
Reliability value W	0.730	0.734	0.735	0.741	0.721	0.729
Failure value Q	0.270	0.261	0.265	0.259	0.279	0.271

It should be noted that the results of the experimental studies and theoretical reliability analysis are fully consistent with the results of the analysis of the consequences of strong earthquakes [27] and the results of the certification of Almaty [28]. Buildings made of monolithic wall structures operated without significant damage under conditions of strong seismic impact.

Table 12 shows the probabilistic characteristics of the reaction parameters of the house, as well as the values of reliability and failure at three values of the coefficient of viscous friction β. The values of β differ by 20% from $\beta = 10$, corresponding to the value of the logarithmic decrement from Section 4.3. The results of **Table 12** allow us to estimate the change in displacement, reliability and failure values when the coefficient of viscous friction changes within the specified limits.

Table 12. Probabilistic reaction parameters for three levels of energy dissipation β, T c/sm.

Parameter	8	10	12
Average displacement, cm	5.443	5.084	4.825
Displacement standard, cm	0.866	0.749	0.664
Average velocity, cm/s	62.080	53.901	48.191
Velocity standard, cm/s	14.659	12.041	10.012
Reliability value, W	0.577	0.735	0.850
Failure value, Q	0.423	0.265	0.150

4.8. Discussion of the research results

This study was designed to solve a practically important problem. Regulatory documents of the Republic of Kazakhstan prohibit the construction of residential buildings above 4 floors in ten-point districts. This building has 6 floors, so it became necessary to conduct a complex of experimental and theoretical studies.

Vibration testing is the only way to create an intense dynamic impact on a full–size building. The method of directional explosions is also used for testing full-scale objects. But in conditions of dense urban development, it is inapplicable.

Vibration effects do not simulate seismic effects. Vibration testing is only a way to bring a natural object into a resonant state. As the intensity of the dynamic effect increases, the resonant frequency or the corresponding oscillation period begins to change. Each intensity of seismic impact in points on the MSK 64(K) Seismic Intensity Scale corresponds to a certain degree of damage to the building. Based on the experimental degree of damage to the building, it is possible to roughly estimate the intensity of the dynamic impact in points. In this scale, a standard spectrum for each magnitude of the seismic impact can be used to assess the intensity of the impact.

After 6 stages of testing with an ever-increasing dynamic load, the building received minor cracks in individual load-bearing and non-load-bearing structures (**Figures 14** and **15**). This is a degree of damage no higher than the first one. The maximum floor skew of the building was 3.07 mm. This is 1/1,000 of the building's floor height. At the same time, the total horizontal load at the 5th stage of the test was 1,020 tf, and at the sixth—758 tf.

We also note that the building is almost completed. All partitions are mounted—the non-load-bearing partitions are shown in **Figures 3** and **4**. The partitions in the building are made of gas blocks with a thickness of 200 mm or 100 mm. There is no interior decoration and facades, but they do not affect the rigidity and damping properties of the building.

Thus, the almost completed building was tested. As a result of the vibration effect, significant horizontal loads were created. The resonant frequencies and oscillation periods are determined. Deformation diagrams are constructed. Under significant horizontal loads, the degree of damage on the MSK-64(K) seismic intensity scale is not higher than the first.

Actually, the test procedure is standard—thousands of buildings have been tested. But the building was designed according to national regulatory documents based on the Eurocode. It is shown that there is a significant margin of bearing capacity. We believe that the building with monolithic reinforced concrete wall structures will ensure the seismic safety of the people living there.

European building codes (Eurocodes) with National annexes that take into account the seismological, climatic and other features of the territory are in force on the territory of the Republic of Kazakhstan. Within the framework of Eurocode 8 "Design of earthquake-resistant structures", the use of a single-mass dynamic model to perform nonlinear calculations is allowed within the framework of the Pushover method. In this case, the movements of the dynamic model are determined. Therefore, it is convenient and logical to accept distortions or movements of the building model in the horizontal direction as a criterion of failure. Based on the analysis of the effects of strong earthquakes, the maximum bias is assumed to be $[x] = h/400 = 0.0025h$. For a single-mass system, h is the height of the building.

Moreover, Section 4.4.3.2 of Eurocode 8 contains restrictions on the misalignment of building floors. For buildings with non-structural elements made of fragile material attached to the structural elements, the maximum bias $[x]v \leq 0.005h$ (v is the responsibility class). For monolithic residential buildings, $v = 0.5$. Therefore, $[x] \leq 0.01h$. This requirement is less stringent than the amount of bias assumed based on the results of the analysis of the effects of strong earthquakes.

It should be noted that Eurocodes are probabilistic in nature. In Eurocode 0, reliability is defined as the probability of uptime. Therefore, it is very logical to perform reliability calculations to quantify the earthquake resistance of a building.

Thus, the reliability calculation is based both on the analysis of earthquake effects and on regulatory documents. Therefore, this calculation was performed correctly.

It should be noted that the results of experimental studies and the theoretical analysis of reliability fully correspond to the results of the analysis of the consequences of strong earthquakes [27] and the results of certification of Almaty city [28]. Buildings made of monolithic wall structures worked without significant damage under conditions of strong seismic impact. The strength of such buildings as a whole is beyond doubt [29,30]. Material costs are reduced and the duration of construction is significantly shortened.

5. Conclusion

The analysis of the vibration test results allows the following principal conclusions to be drawn.

a) The experimental data obtained confirm the validity of the adopted building calculation model. The identified differences in the calculated and experimental values of the vibration periods are explained by the reasons listed in Section 4.

b) The maximum horizontal inertial forces impacting on the experimental object in the transverse direction along the fundamental vibration mode amounted to 84.78% of the calculated 10-point loads;
c) The relatively small values of the coefficient μ corresponding to test stages III–VI indicate significant reserves of the test object's capacity to develop plastic deformations.
d) The maximum horizontal distortions of the floors did not exceed 3.07 mm, the maximum irregularity in plan did not exceed 2.1%, and the maximum irregularity in height did not exceed 1.03. Based on the test results, the building is classified as regular in plan and regular in height.
e) After VI stages of vibration testing, minor cracks formed in individual load-bearing and non-load-bearing structures.
f) The actual condition of the building after vibration testing is fully consistent with the condition stipulated by the scientific and methodological principles of the current regulations "Construction in Seismic Zones."
g) Based on the results of the visual inspection, it is recommended to rectify the identified defects.
h) No data indicating insufficient seismic resistance of the 6-story building was obtained during the vibro-dynamic testing.
i) Analysis of seismic resistance based on reliability values W shows that seismic resistance is ensured with a fairly high probability.

Author contributions: Conceptualization, VL, YA and ZO; methodology, VL and YA; validation, YA and KT; formal analysis, VL and KT; investigation, VL; resources, YA and KT; data curation, KT; writing—original draft preparation, ZO and KT; writing—review and editing, YA; visualization, KT; supervision, KT; project administration, VL and ZO; funding acquisition, VL. All authors have read and agreed to the published version of the manuscript.

Funding: This research is funded by the Committee of Science of the Ministry of Science and Higher Education of the Republic of Kazakhstan (Grant No. BR24992763). The research was also carried out within the framework of the project "Assessment of the Seismogeodynamic State of the Almaty Agglomeration Based on Monitoring of Seismic, Geophysical, and Hydrogeochemical Parameters", implemented with the support of the Akimat of Almaty.

Institutional review board statement: Not applicable.

Informed consent statement: Not applicable.

Data availability statement: The data are available from the authors upon reasonable request.

Conflict of interest: The authors declare no conflict of interest.

AI use statement: The authors declare that no artificial intelligence (AI) tools were used in the preparation of this manuscript.

References

1. Atmaca B, Altunişik AC, Ertürk Atmaca E, et al. What is the reason for collapses on February 6, 2023 Kahramanmaraş earthquakes: Insights from a dataset of 400 collapsed RC buildings post-earthquake analysis. Journal of Building Engineering. 2025; 107: 112660. doi: 10.1016/j.jobe.2025.112660
2. Öztürk M, Arslan MH, Doğan G, et al. School buildings performance in 7.7 Mw and 7.6 Mw catastrophic earthquakes in southeast of Turkey. Journal of Building Engineering. 2023; 79: 107810. doi: 10.1016/j.jobe.2023.107810
3. Caldeira B, Muñoz CP, Oliveira RJ, et al. Analysis of the 8 September 2023 Al Haouz (Morocco) earthquake source using seismic and geodetic data. Journal of Seismology. 2026; 30(1): 3. doi: 10.1007/s10950-025-10357-1
4. Boulanouar A, Tiwari RK, Ahmed Z, et al. Fractal characteristics of earthquake occurrence in Al Hoceima city and its adjoining region, Morocco. Geosystems and Geoenvironment. 2025; 4(3): 100402. doi: 10.1016/j.geogeo.2025.100402
5. Fu J, Chen Y, Nie Q, et al. Source modeling of the 2023 Herat earthquake sequence determined from InSAR observations. Geodesy and Geodynamics. 2025; 16(5): 624–634. doi: 10.1016/j.geog.2025.01.003
6. Hou H, Ji L, Zhu L, et al. InSAR deformation observation and seismogenic tectonic analysis of the 2025 Mw 6.0 Afghanistan earthquake. Geodesy and Geodynamics. 2026; in press. doi: 10.1016/j.geog.2026.04.008
7. Shapiro GA, Simon YA, Ashkinadze GN, et al. Vibration Testing of Buildings. Stroyizdat; 1972. (in Russian)
8. Zolotkov AS. Seismic Stability of Monolithic Buildings. Kartya Moldovey; 2000. (in Russian)
9. Zolotcov AS. Vibration tests on fragments of monolithic building until destruction. Magazine of Civil Engineering. 2012; 27(1): 14–21. doi: 10.5862/MCE.27.2 (in Russian)
10. Tuleyev A, Omarov Z, Abakanov T, et al. Vibration test of a high-rise monolithic building. International Journal of GEOMATE. 2023; 25(109): 149–156. doi: 10.21660/2023.109.m2315
11. Hadianfard MA, Jahangiri M, Shojaei S. The effects of non-structural components on the dynamic characteristics and vulnerability of concrete structures using ambient vibration tests and Nakamura's criterion. Soil Dynamics and Earthquake Engineering. 2022; 162: 107492. doi: 10.1016/j.soildyn.2022.107492
12. Yang Z, Jian M, Lin Y, et al. A study on the formula of fundamental period of high-rise shear wall structures based on ambient vibration testing. Structures. 2024; 64: 106622. doi: 10.1016/j.istruc.2024.106622
13. Kanbara S, Shaw R, Eguchi K, et al. Lessons from the 2024 Noto Peninsula Earthquake: Need for digital transformation in disaster response. Progress in Disaster Science. 2025; 25: 100400. doi: 10.1016/j.pdisas.2024.100400
14. Mkrtychev OV, Raiser VD. Reliability Theory in the Design of Building Structures. ASV Publishing House; 2016. (in Russian)
15. Bolotin VV. Statistical Methods in Structural Mechanics. Holden-Day; 1969.
16. Lapin V, Shokbarov Y, Aldakhov Y. The buildings' reliability calculating method using a simple seismic impact model. Civil Engineering Journal. 2024; 10(8): 2734–2744. doi: 10.28991/CEJ-2024-010-08-019
17. Aldakhov Y, Lapin V, Moldamuratov Z, et al. Statistical estimation of reliability values for large-panel buildings based on passportization results. Civil Engineering Journal. 2025; 11(5): 2066–2083. doi: 10.28991/CEJ-2025-011-05-019
18. Hurtado JE, Barbat AH. Monte Carlo techniques in computational stochastic mechanics. Archives of Computational Methods in Engineering. 1998; 5: 3–29. doi: 10.1007/BF02736747
19. Hofer L, Toska K, Zanini MA, et al. The influence of the seismic hazard and structural fragility related uncertainties on the seismic reliability. Procedia Structural Integrity. 2026; 78: 1927–1934. doi: 10.1016/j.prostr.2025.12.245
20. Shen J, Pan J, Ding G, et al. Seismic reliability analysis of frame structure subjected to sequential ground motions using probability density evolution method. Journal of Building Engineering. 2025; 112: 113667. doi: 10.1016/j.jobe.2025.113667
21. Brenner CE, Bucher C. A contribution to the SFE-based reliability assessment of nonlinear structures under dynamic loading. Probabilistic Engineering Mechanics. 1995; 10(4): 265–273. doi: 10.1016/0266-8920(95)00021-6
22. Sadykova AB, Silacheva NV, Stepanenko NP. Seismic micro zoning of the territory of Almaty on a new methodological basis. News of the National Academy of Sciences of the Republic of Kazakhstan, Series of Geology and Technical Sciences. 2021; 1(445): 127–134. doi: 10.32014/2021.2518-170X.18
23. Kopnichev YF, Sokolova IN. Heterogeneities of the shear wave attenuation field in the lithosphere of

East Tien Shan and their relationship with seismicity. Doklady Earth Sciences. 2012; 442: 292–295. doi: 10.1134/S1028334X12020249
24. KazNIISA JSC. Code of Practice of the Republic of Kazakhstan 2.03-31-2020: Development of the Territory of Almaty Taking into Account Seismic Microzoning. Publishing Department of KazNIISA JSC; 2020. (in Russian)
25. KazNIISA JSC. Code of Practice of the Republic of Kazakhstan 2.03-30-2017: Construction in Seismic Zones. Publishing Department of KazNIISA JSC; 2018. (in Russian)
26. Mkrtychev OV, Yuriev RV. Modeling of Random Accelerograms and Nonlinear Calculation of Building Structures. Moscow State University of Civil Engineering; 2012. (in Russian)
27. Vicente R, Ferreira T, Maio R. Seismic risk at the urban scale: Assessment, mapping and planning. Procedia Economics and Finance. 2014; 18: 71–80. doi: 10.1016/S2212-5671(14)00915-0
28. Rashid MS, Zhang D, Moon SW, et al. Macro-seismic assessment for residential buildings constructed in the Soviet Union era in Almaty, Kazakhstan. Buildings. 2023; 13(4): 1053. doi: 10.3390/buildings13041053
29. Grünthal G (editor). European Macroseismic Scale 1998 (EMS-98). Centre Européen de Géodynamique et de Séismologie; 1998.
30. Chopra AK. Dynamics of Structures: Theory and Applications to Earthquake Engineering. Prentice-Hall; 1995.